

Supporting Information

Continuous Flow Solvent-Free and Catalyst-Free Mechanochemical Production of Rhodamine-B Dyes and its Derivatives

Mukesh Purohit^{ab}, Tabrez Rafique Shaikh^{ab} and Amol A. kulkarni^{*ab}

- a)** Chemical Engineering & Process Development, CSIR-National Chemical Laboratory
Pune, 411008, India. E-mail: aa.kulkarni@ncl.res.in
- b)** Academy of Scientific and Innovative Research (AcSIR), Ghaziabad, Uttar pradesh
201002, India.

Table of Contents

Content	Page #
General Methods	S3
Comparison Table With Previous Work	S3
General Reaction Procedure	S4
Experimental setup for Rhodamine-b and its Derivatives by using Screw Reactor	S4
Details of the Screw Reactor	S5
Uv-Visible, PL and PLQY Spectroscopy Data	S5
¹ H NMR and ¹³ C NMR Spectra of Compounds (Characterization Data)	S8
¹ H NMR and ¹³ C NMR Spectra of Compounds (Spectroscopic Data)	S11
HRMS(High-resolution mass spectrometry) data of compound	S17
References	S20

General Methods

All reagents and solvents used in this study were of commercial grade and were utilized without further purification. The reactions were conducted in a single-screw Teflon reactor at a temperature of 180 °C. Reaction progress was monitored via thin-layer chromatography (TLC) using Merck silica gel 60-F254 plates (0.25 mm thickness), with detection carried out under UV light. UV-Vis absorption spectra were recorded at room temperature using an Agilent Technologies 8453 UV-Vis spectrophotometer, which operates with a single beam in the wavelength range of 190–1100 nm and provides a measurement accuracy of ± 0.5 nm. Yields reported corresponding to isolated, spectroscopically pure compounds. ^1H and ^{13}C NMR spectra were obtained using a Bruker instrument operating at 400 MHz and 500 MHz, respectively, with tetramethylsilane (TMS) as the internal standard. Chemical shifts are reported in parts per million (ppm, δ) relative to TMS for ^1H NMR and to the ^{13}C resonance of CDCl_3 (77.0 ppm). NMR data are presented in the following format: chemical shift (δ), multiplicity [s = singlet, d = doublet, t = triplet, m = multiplet, b = broad], coupling constant (J, Hz), and integration values.

Table: 1 Comparison with previous work:

Serial No	Used catalyst	Temperature (°C)	Reaction Time	Yield	Compound	process	Reference
1	H^+	175	3-5 hr	Low yield	Rhodamine-b	batch	¹
2	H_2SO_4	180	6 hr	63 %	Rhodamine derivative	batch	²
3	H_2SO_4	150	2 hr	–	Rhodamine-b	batch	³
4	H_2SO_4	150	20-30 min	21-73%	Rhodamine derivative	Microwave batch	⁴
5	$\text{CH}_3\text{SO}_3\text{H}$	110	17 hr	49 %	Rhodamine derivative	batch	⁵
6	H_2SO_4	25 Hz (Ball milling Process)	3 hr	95 %	Rhodol derivative	batch	⁶
7	Nb_2O_5	180	1 hr	85 %	Rhodamine-b	batch	⁷
8	Without catalyst	180	12 min	79 %	Rhodamine-b	Continuous flow	This work

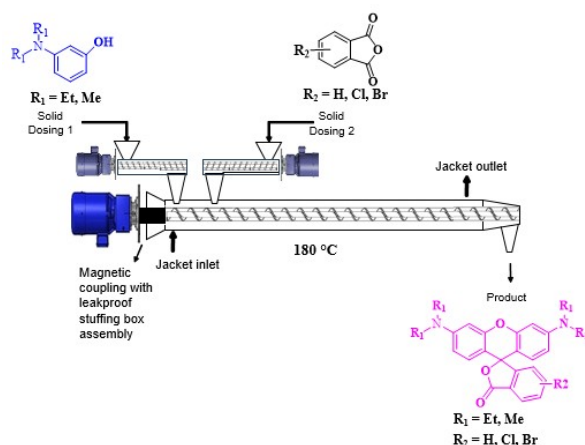
General experimental procedure Note:

Upon completion of the reaction, as verified by thin-layer chromatography (TLC), the residual product present in the grooves of the screw reactor was extracted using the appropriate solvents utilized during the reaction. This was followed by vacuum evaporation to minimize any potential loss in product yield.

General procedure for continuous flow synthesis of Rhodamine by mechanochemical approach.

N,N-Diethyl-3-aminophenol (1) (0.027 mol, 2 equivalents) was introduced at a flow rate of 0.84 mL/min from solid dosing unit 1, while phthalic anhydride (3) (0.0135 mol, 1 equivalent) was fed at a flow rate of 0.25 mL/min from solid dosing unit 2 into a screw reactor rotating at 30-45 rpm, with the temperature maintained at approximately 180 °C. The total residence time for the formation of Rhodamine and its derivatives was 10-12 minutes. A colored solid product was collected and monitored by thin-layer chromatography (TLC) using a solvent system of acetone: petroleum ether (9:1) to track the formation of the desired products. TLC analysis indicated the presence of some impurities formed during the reaction. The crude residue was purified by column chromatography on silica gel (petroleum ether: Acetone: 3:7) to yield **1a** (79%) as a purple solid. However, the complete isolation of all impurities was challenging, with some minor impurities remaining unresolved. All products were characterized using ¹H and ¹³C NMR spectroscopic techniques, and their molecular masses were confirmed by high-resolution mass spectrometry (HRMS).

General experimental setup for Rhodamine and its derivatives by using screw reactor:



Details of the screw reactor:

A jacketed single-screw reactor (glass-Teflon) have used for continuous flow mechanochemical synthesis of Rhodamine-b. We have purchased a glass-Teflon reactor. which allows us to monitor the changes occurring visibly during the course of the reaction. The extruder was fabricated by M/s Alpro Pvt. Ltd., Pune (India), and the vertical alignment for the screw reactor (having a glass jacket with a 50 mm outer diameter and 20.5 mm inner diameter and a 460 mm long PTFE screw with a 20 mm diameter). This leaves a gap of only 0.25 mm between the jacket wall and the screw threads, the screw reactor, as shown in Figure 1. The inlet and outlet ports of the jacket are connected to a constant temperature circulation bath (julabo, Germany). The residence time was controlled using the rotation speed of the screw, controlled using a precision motor (Remi, India). The screw reactor parameters can be tuned to optimize the process for the Rhodamine-b synthesis with good to excellent yield with short residence time, including the screw profile, feed rate, screw speed, and temperature.

Uv, PL, and PLQY measurements: Steady state PL measurements were performed using a spectrofluorometer (FS5, Edinburgh Instrument) coupled with a Hamamatsu NIR PMT module controller (H10330C-75-C3). An integrating sphere (SC-30) attached to the spectrofluorometer was used for PLQY measurement using the software provided by the manufacturer.

Uv-Visible spectroscopy data

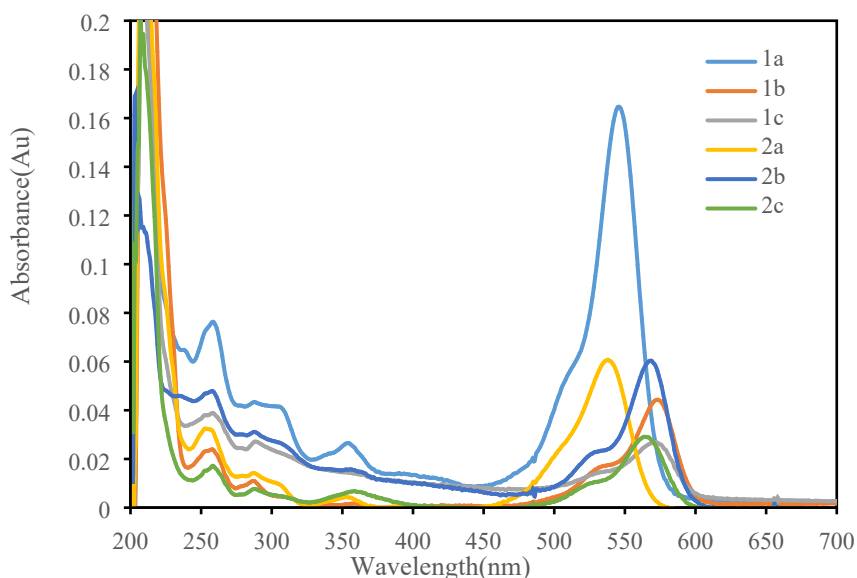


Figure 1: Uv-visible absorbance of all compounds in Methanol

The effect of substituent groups was investigated in methanol, revealing that a slight increase in the carbon chain length of the amine group (from methyl to ethyl) results in a noticeable change in the emission color. When compared to the halogen-free derivatives, the chlorinated and brominated derivatives (1b and 2b) as well as (1c and 2c) exhibit a bathochromic shift, indicating a shift towards longer wavelengths in their emission spectra.

Fluorescence Spectroscopy data

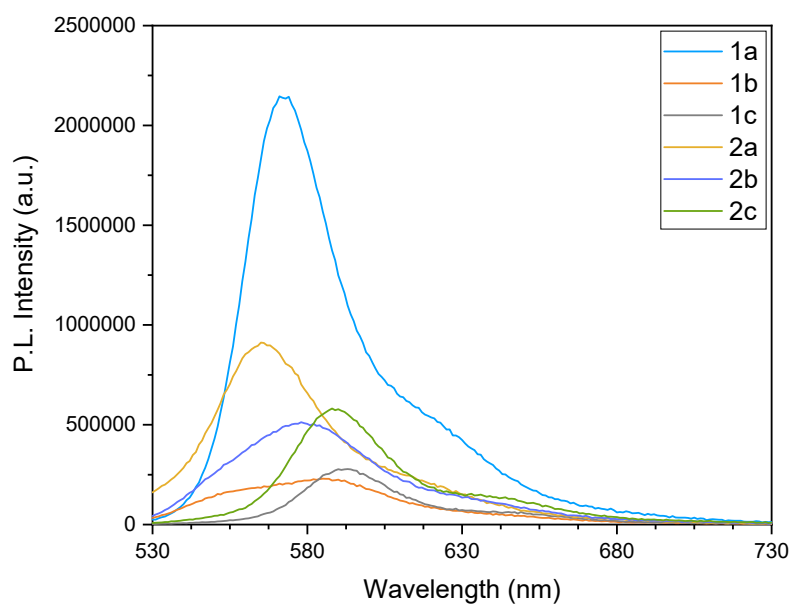


Figure 2: Fluorescence spectra for all compounds in methanol

Photoluminescence Quantum Yield (PLQY): Quantum yield was measured in the above mentioned instrument. All quantum yield is mentioned in the graph below.

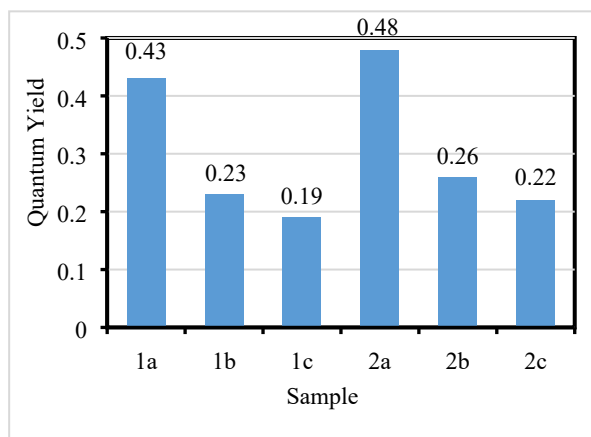


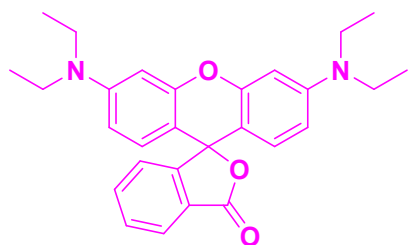
Figure 3: Photoluminescence Quantum Yield

According to the PLQY data, non-halogenated Rhodamine-B derivatives (1a and 2a) exhibit a higher quantum yield compared to their chlorinated and brominated counterparts (1b, 1c, 2b, and 2c), indicating that the non-halogenated forms more efficiently convert absorbed photons into emitted light. Due to this higher photoluminescent quantum yield, derivatives 1a and 2a are particularly suitable for applications in fluorescent probes and sensors⁸, light-emitting diodes (LEDs)⁹, laser dyes¹⁰, and solar cells¹¹, where strong fluorescence and efficient light emission are essential for performance.

Spectral data of the synthesized compounds

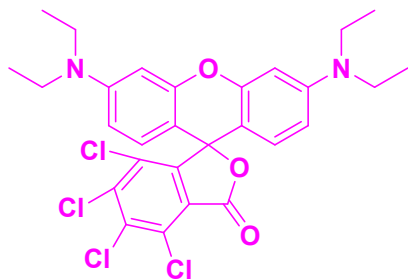
Characterization Data:

3',6'-bis(diethylamino)-3H-spiro[isobenzofuran-1,9'-xanthen]-3-one. (1a)



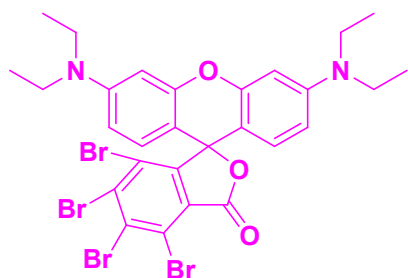
(Purple solid, 79%), ^1H NMR (500 MHz, CHLOROFORM-*d*): δ ppm 1.18 (t, $J=7.07$ Hz, 12 H, CH₃) 3.36 (q, $J=7.00$ Hz, 8 H, CH₂) 6.33 (dd, $J=8.94, 2.69$ Hz, 2 H, Ar-H) 6.42 - 6.48 (m, 2 H, Ar-H) 6.56 (d, $J=8.88$ Hz, 2 H, Ar-H) 7.22 (d, $J=7.38$ Hz, 1 H, Ar-H) 7.54 - 7.67 (m, 2 H, Ar-H) 7.96 - 8.03 (m, 1 H, Ar-H). ^{13}C NMR (101 MHz, CHLOROFORM-*d*) δ = 169.9, 153.3, 153.2, 149.5, 134.4, 129.1, 128.9, 127.9, 124.7, 124.2, 108.0, 105.9, 97.6, 86.0, 44.5, 12.6 HRMS (ESI): (M+H)⁺ Calcd for C₂₈H₃₁N₂O₃ 443.56, found 443.23

4,5,6,7-tetrachloro-3',6'-bis(diethylamino)-3H-spiro[isobenzofuran-1,9'-xanthen]-3-one. (1b)



(Purple solid, 75%), ^1H NMR (500 MHz, CDCl₃) ^1H NMR (500 MHz, CHLOROFORM-*d*) δ ppm 1.20 (t, $J=7.07$ Hz, 12 H, CH₃) 3.38 (q, $J=7.13$ Hz, 8 H, CH₂) 6.36 - 6.42 (m, 2 H, Ar-H) 6.42 - 6.47 (m, 2 H, Ar-H) 6.66 (d, $J=8.75$ Hz, 2 H, Ar-H). ^{13}C NMR (101 MHz, CHLOROFORM-*d*) δ = 165.7, 157.0, 152.5, 149.0, 134.2, 129.2, 127.6, 126.9, 121.2, 118.9, 107.3, 104.4, 96.6, 84.5, 43.5, 11.5 HRMS (ESI): (M+H)⁺ Calcd for C₂₈H₂₇N₂O₃Cl₄ 579.0770, found 579.0761

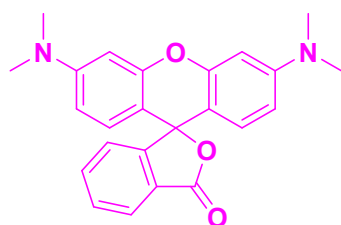
4,5,6,7-tetrabromo-3',6'-bis(diethylamino)-3H-spiro[isobenzofuran-1,9'-xanthen]-3-one. (1c)



(Purple solid, 72%), ^1H NMR (500 MHz, CDCl_3): ^1H NMR (400 MHz, $\text{CHLOROFORM-}d$) δ ppm 1.19 (t, $J=7.07$ Hz, 12 H, CH_3) 3.37 (q, $J=7.05$ Hz, 8 H, CH_2) 6.37 (d, $J=8.75$ Hz, 2 H, Ar-H) 6.41 - 6.44 (m, 2 H, Ar-H) 6.61 (d, $J=8.88$ Hz, 2 H, Ar-H). ^{13}C NMR (101 MHz, $\text{CHLOROFORM-}d$) δ = 164.8, 153.7, 149.9, 147.8, 135.3, 132.5, 129.7, 128.6, 127.9, 126.4, 108.3, 104.8, 97.6, 84.1, 44.5, 12.5

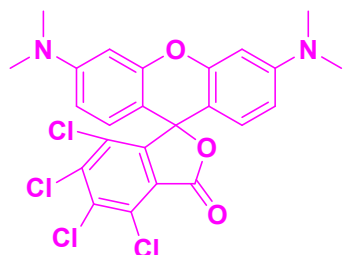
HRMS (ESI): $(\text{M}+\text{H})^+$ Calcd for $\text{C}_{28}\text{H}_{27}\text{N}_2\text{O}_3\text{Br}_2$ 758.8709, found 754.8689

3',6'-bis(dimethylamino)-3H-spiro[isobenzofuran-1,9'-xanthen]-3-one. (2a)



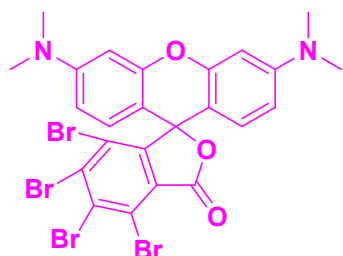
(Purple solid, 84%), ^1H NMR (500 MHz, $\text{CHLOROFORM-}d$) δ ppm 2.99 (s, 12 H, CH_3) 6.40 (dd, $J=8.94, 2.69$ Hz, 2 H, Ar-H) 6.50 (d, $J=2.63$ Hz, 2 H, Ar-H) 6.61 (d, $J=8.75$ Hz, 2 H, Ar-H) 7.16 - 7.21 (m, 1 H, Ar-H) 7.55 - 7.68 (m, 2 H, Ar-H) 7.97 - 8.04 (m, 1 H, Ar-H). ^{13}C NMR (101 MHz, $\text{CHLOROFORM-}d$) δ = 169.9, 153.3, 153.2, 149.5, 134.4, 129.1, 128.9, 127.9, 124.7, 124.2, 108.0, 105.9, 97.6, 86.0, 44.5 HRMS (ESI): $(\text{M}+\text{H})^+$ Calcd for $\text{C}_{24}\text{H}_{23}\text{N}_2\text{O}_3$ 387.1703, found 387.1694

4,5,6,7-tetrachloro-3',6'-bis(dimethylamino)-3H-spiro[isobenzofuran-1,9'-xanthen]-3-one. (2b)



(Purple solid, 78%), ^1H NMR (500 MHz, CHLOROFORM-*d*) δ ppm 3.01 (s, 12 H, CH₃) 6.43 (dd, $J=8.82, 2.56$ Hz, 2 H, Ar-H) 6.47 (d, $J=2.50$ Hz, 2 H, Ar-H) 6.67 (d, $J=8.76$ Hz, 2 H, Ar-H). ^{13}C NMR (101MHz, CHLOROFORM-*d*) $\delta=$ 168.2, 153.0, 152.3, 149.7, 139.9, 135.4, 128.6, 127.6, 123.8, 108.7, 103.2, 98.5, 91.7, 83.9, 40.2 HRMS (ESI): (M+H)⁺ Calcd for C₂₄H₁₉N₂O₃Cl₃³⁷Cl 525.0115, found 525.0120

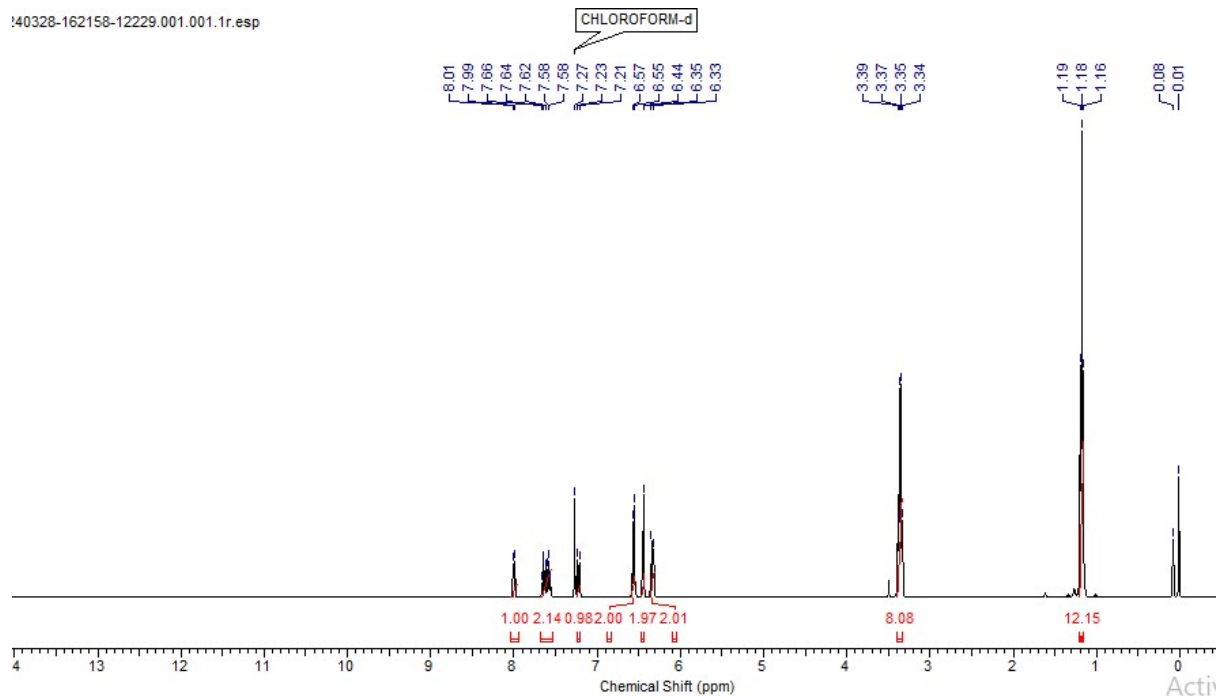
4,5,6,7-tetrabromo-3',6'-bis(dimethylamino)-3H-spiro[isobenzofuran-1,9'-xanthen]-3-one. (2c)



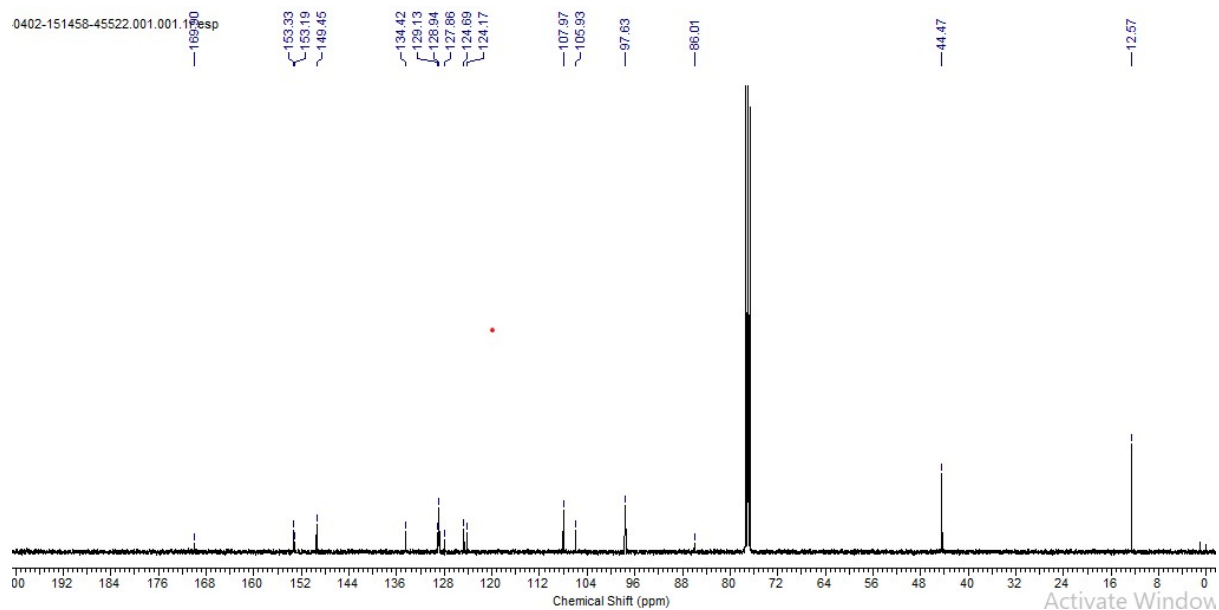
(Purple solid, 76%), ^1H NMR (500 MHz, CHLOROFORM-*d*) δ ppm 2.92 (s, 12 H, CH₃) 6.32 - 6.36 (m, 2 H, Ar-H) 6.38 (d, $J=2.63$ Hz, 2 H, Ar-H) 6.56 (d, $J=8.76$ Hz, 2 H, Ar-H). ^{13}C NMR (101MHz, CHLOROFORM-*d*) $\delta =$ 164.8, 153.2, 152.2, 148.1, 137.2, 132.3, 127.7, 126.4, 122.6, 122.1, 108.7, 103.3, 98.4, 91.8, 40.2 HRMS (ESI): (M+H)⁺ Calcd for C₂₄H₁₉N₂O₃Br₂⁸¹Br₂ 702.8063, found 702.8083

Spectroscopic Data:

¹H NMR- of 3',6'-bis(diethylamino)-3H-spiro[isobenzofuran-1,9'-xanthen]-3-one. (1a)

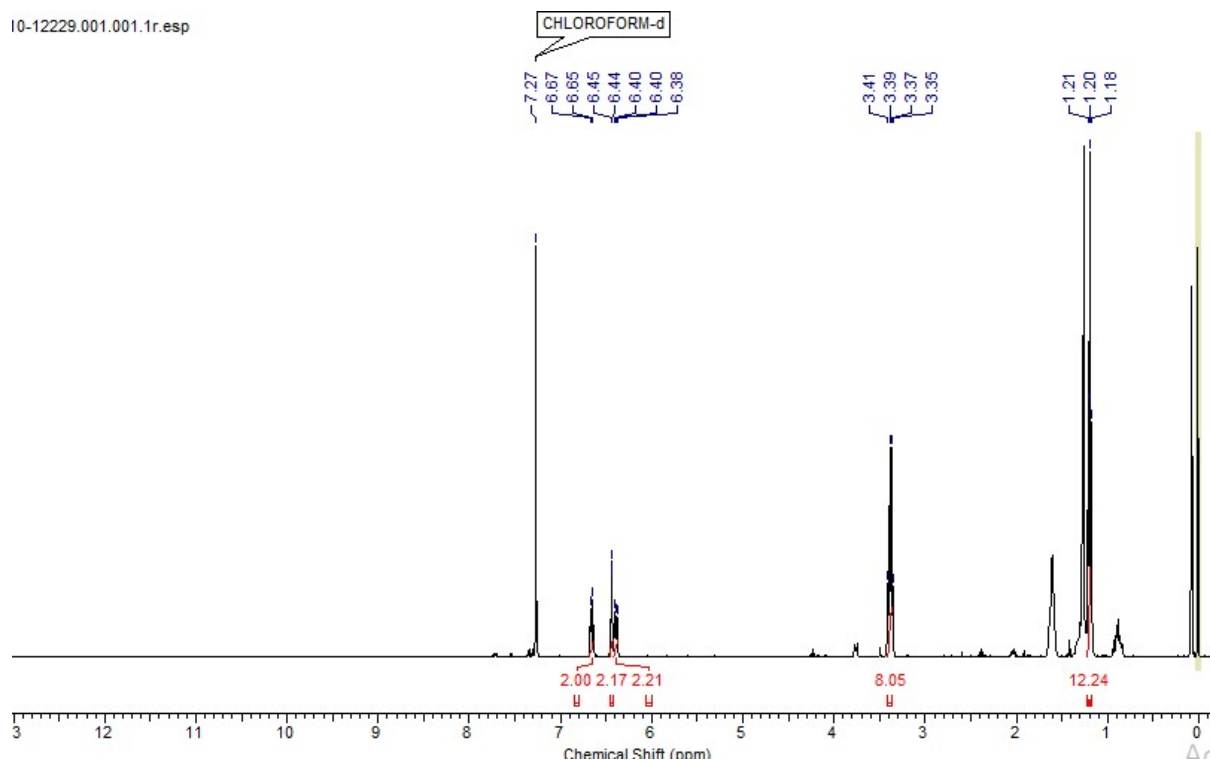


¹³C NMR- of 3',6'-bis(diethylamino)-3H-spiro[isobenzofuran-1,9'-xanthen]-3-one. (1a)

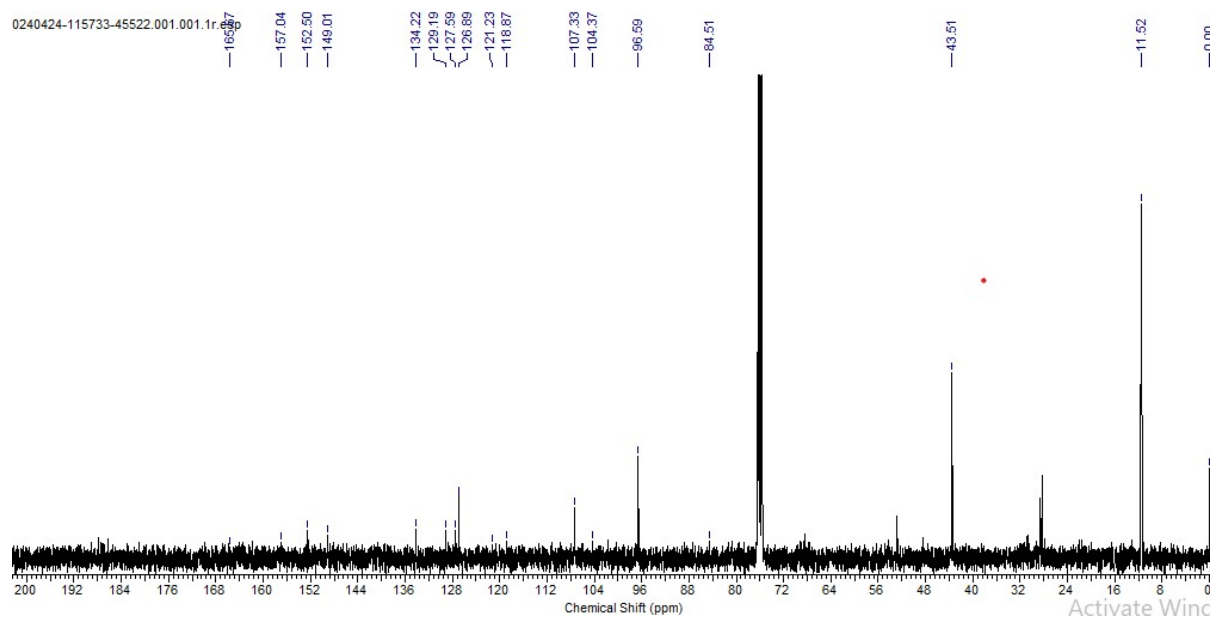


¹H NMR- of 4,5,6,7-tetrachloro-3',6'-bis(diethylamino)-3H-spiro[isobenzofuran-1,9'-xanthen]-3-one. (1b)

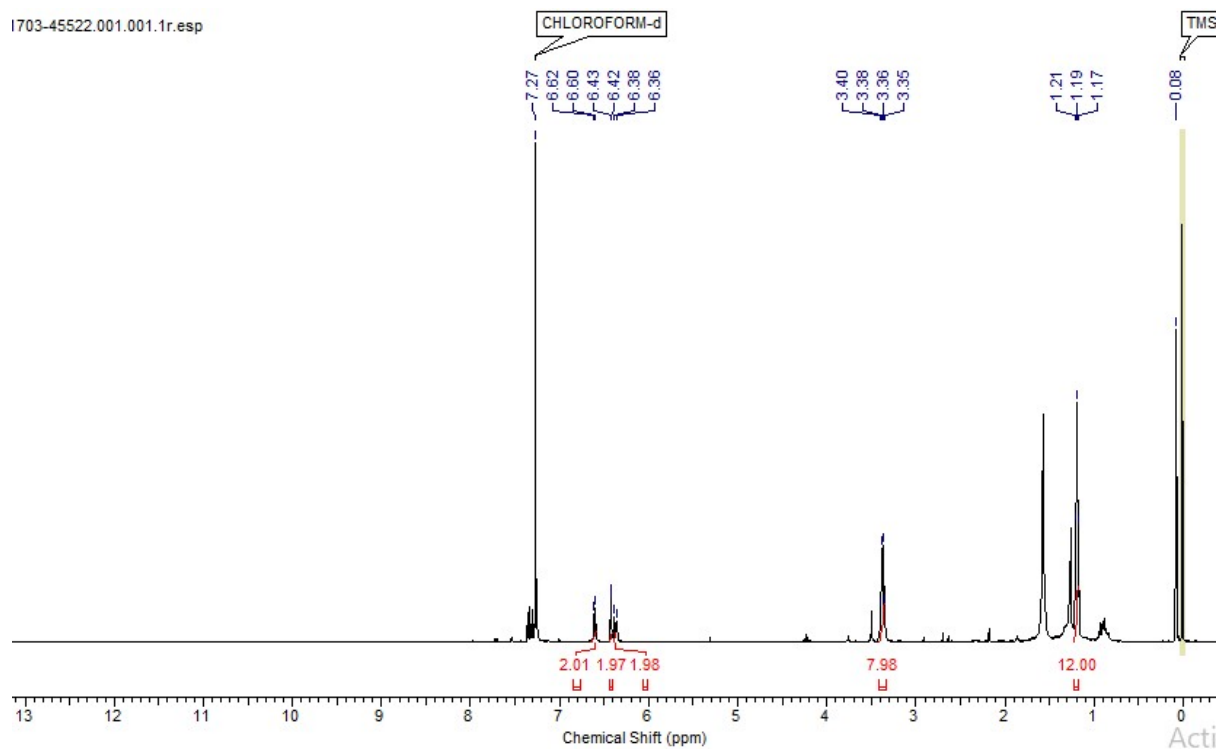
10-12229.001.001.1r.esp



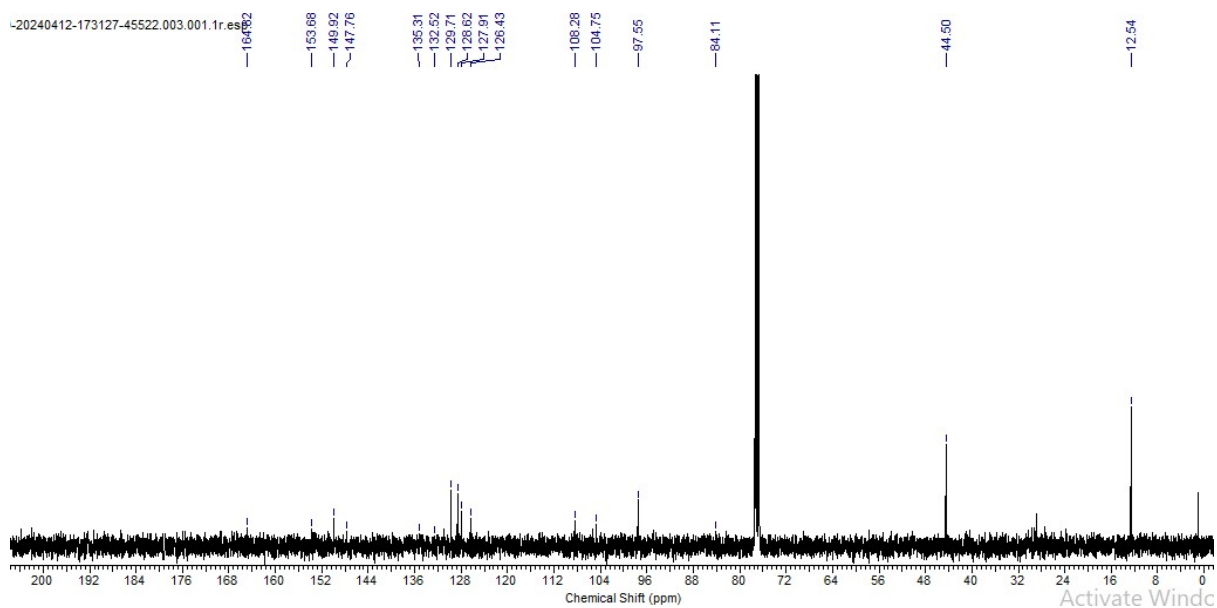
¹³C NMR- of 4,5,6,7-tetrachloro-3',6'-bis(diethylamino)-3H-spiro[isobenzofuran-1,9'-xanthen]-3-one. (1b)



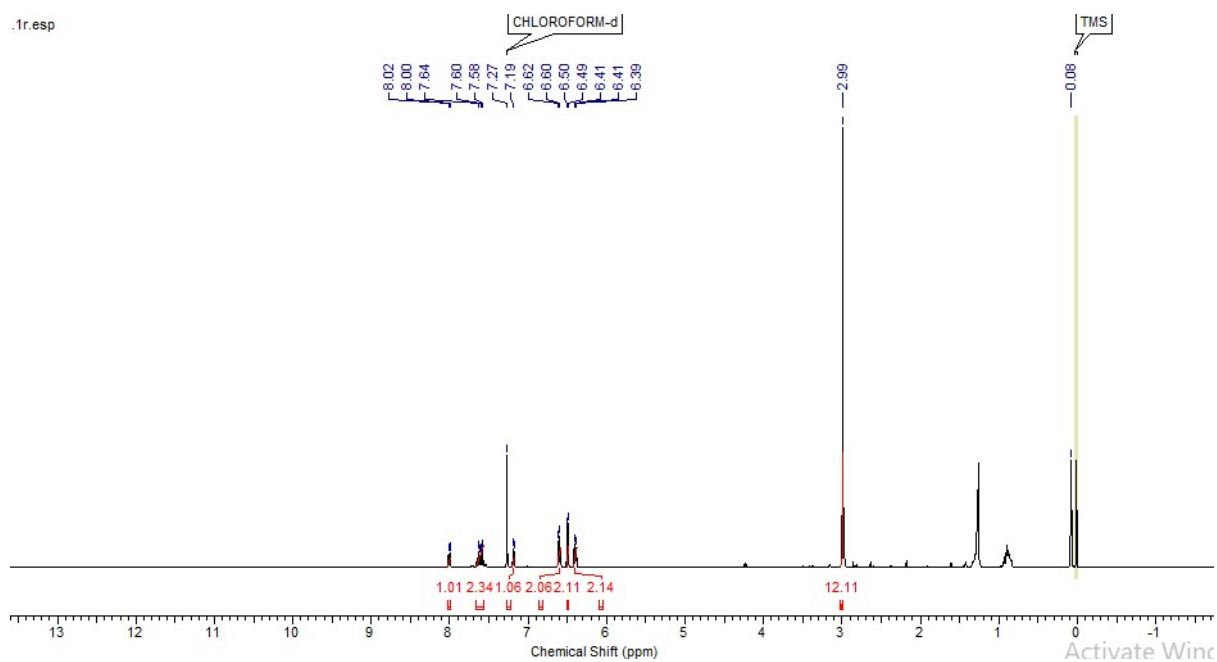
¹H NMR- of 4,5,6,7-tetrabromo-3',6'-bis(diethylamino)-3H-spiro[isobenzofuran-1,9'-xanthen]-3-one. (1c)



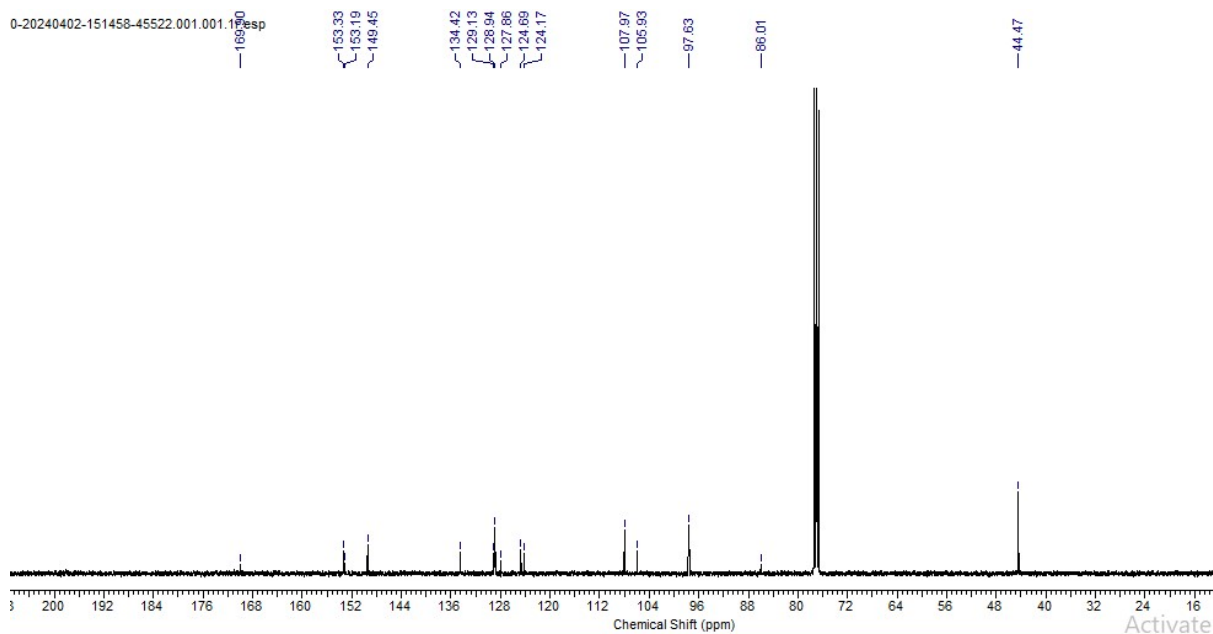
¹³C NMR- of 4,5,6,7-tetrabromo-3',6'-bis(diethylamino)-3H-spiro[isobenzofuran-1,9'-xanthen]-3-one. (1c)



¹H NMR- of 3',6'-bis(dimethylamino)-3H-spiro[isobenzofuran-1,9'-xanthen]-3-one. (2a)

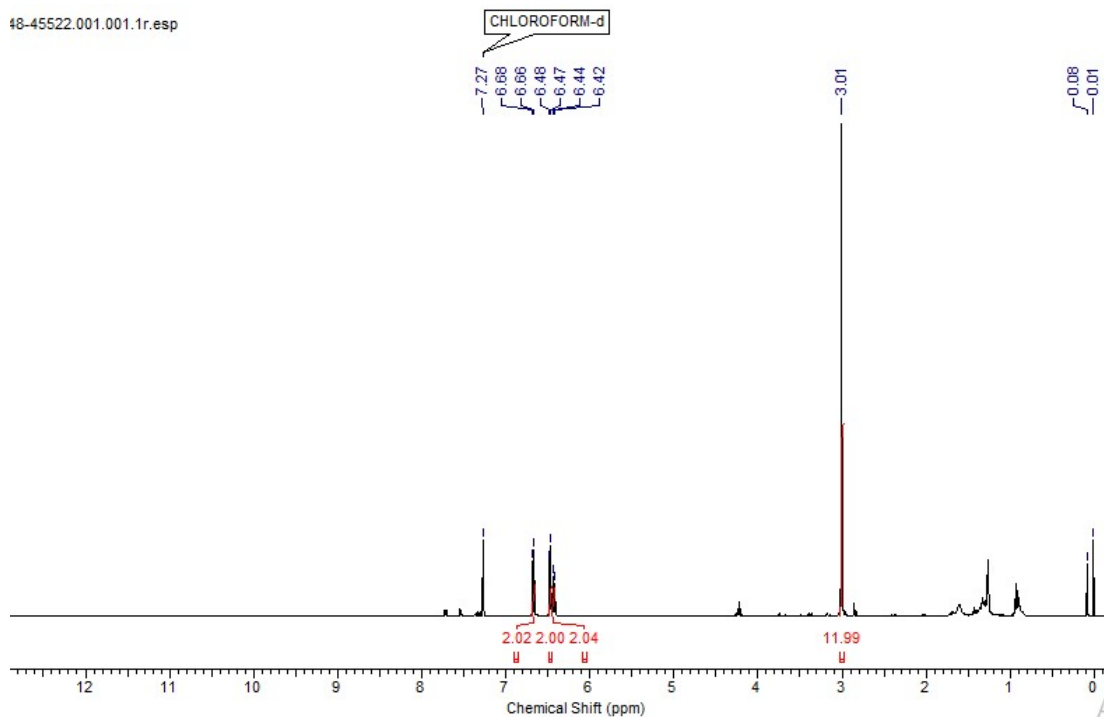


¹³C NMR- of 3',6'-bis(dimethylamino)-3H-spiro[isobenzofuran-1,9'-xanthen]-3-one. (2a)

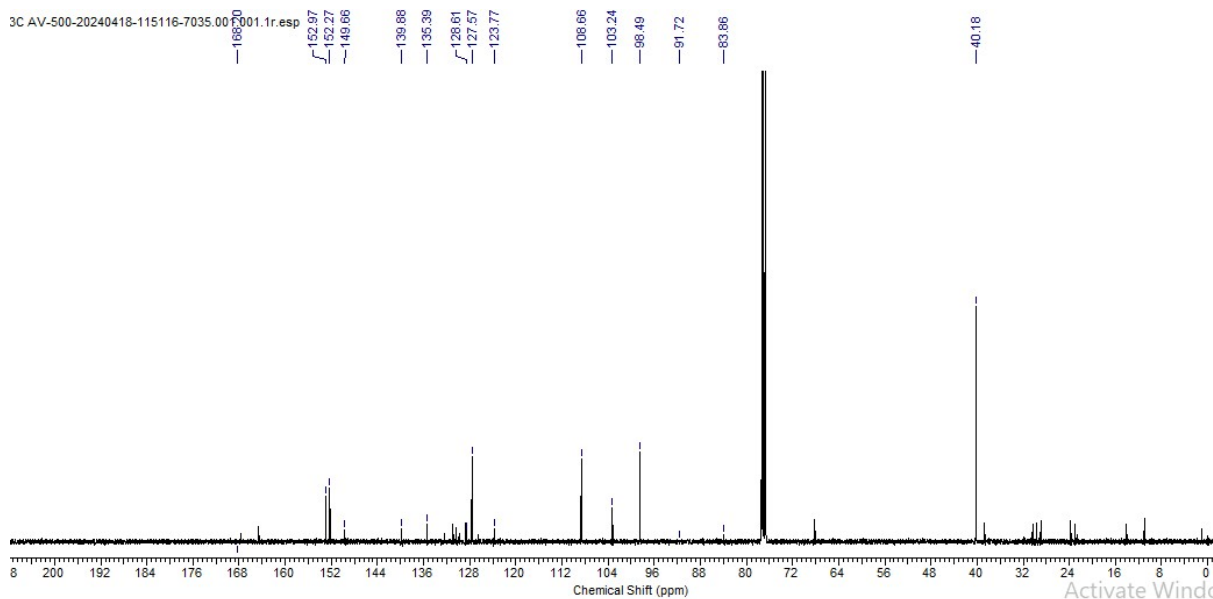


¹H NMR- of 4,5,6,7-tetrachloro-3',6'-bis(dimethylamino)-3H-spiro[isobenzofuran-1,9'-xanthen]-3-one. (2b)

48-45522.001.001.1r.esp

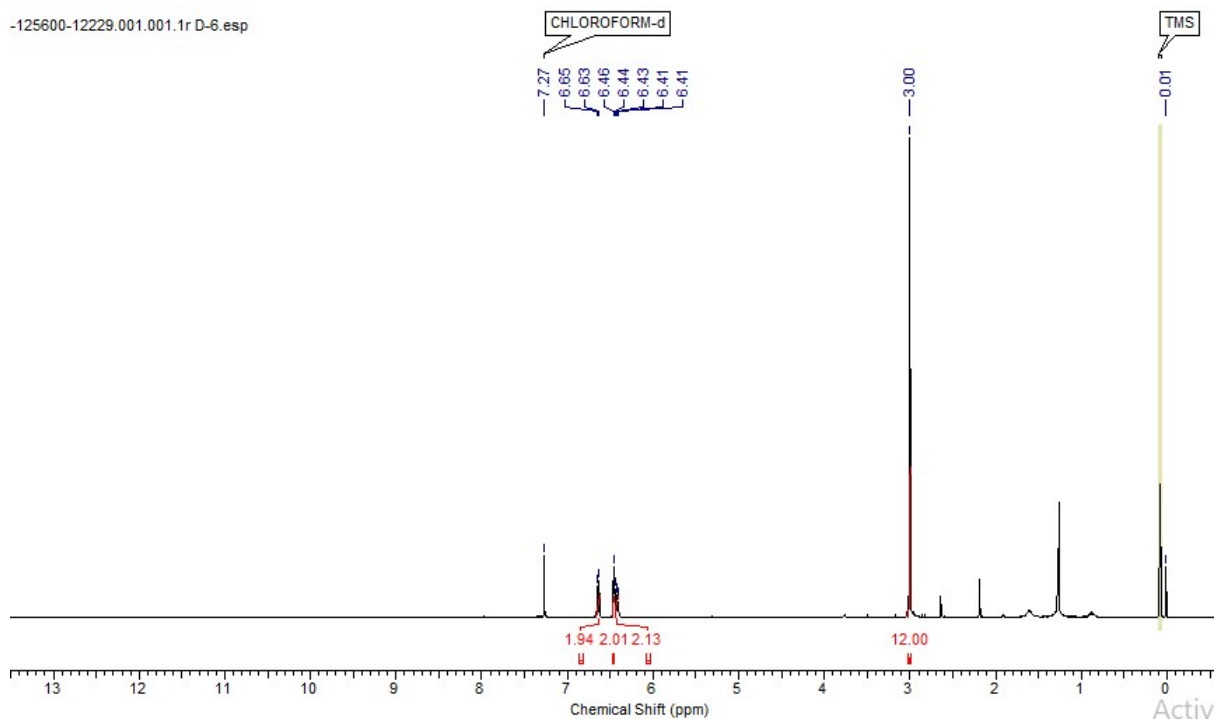


¹³C NMR- of 4,5,6,7-tetrachloro-3',6'-bis(dimethylamino)-3H-spiro[isobenzofuran-1,9'-xanthen]-3-one. (2b)

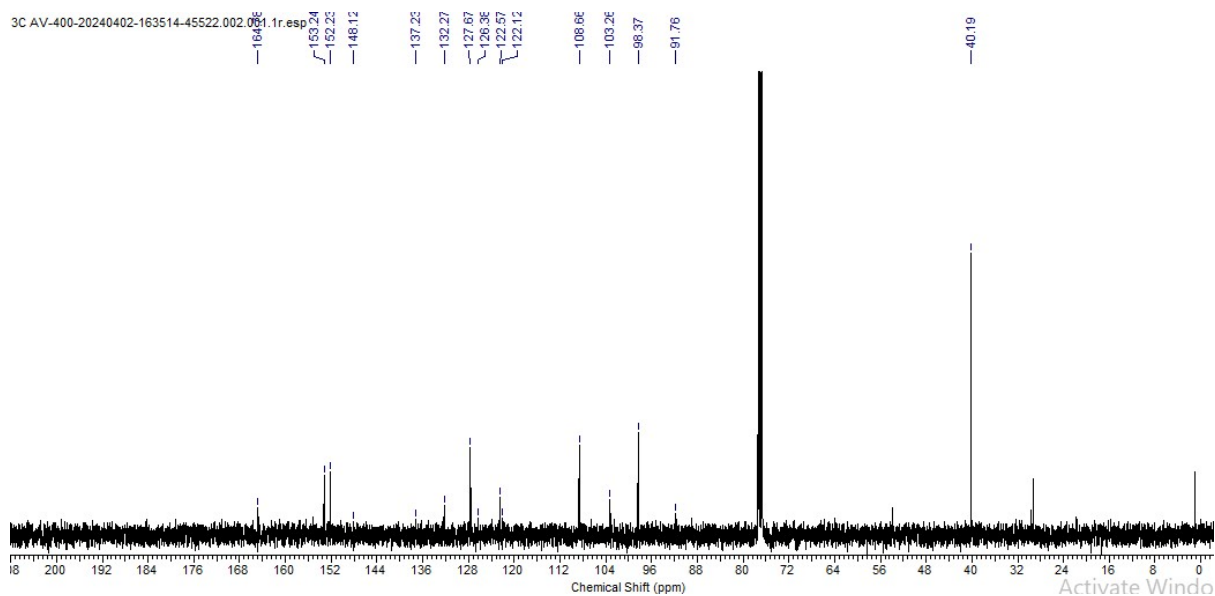


¹H NMR- of 4,5,6,7-tetrachloro-3',6'-bis(dimethylamino)-3H-spiro[isobenzofuran-1,9'-xanthen]-3-one. (2c)

-125600-12229.001.001.1r D-6.esp

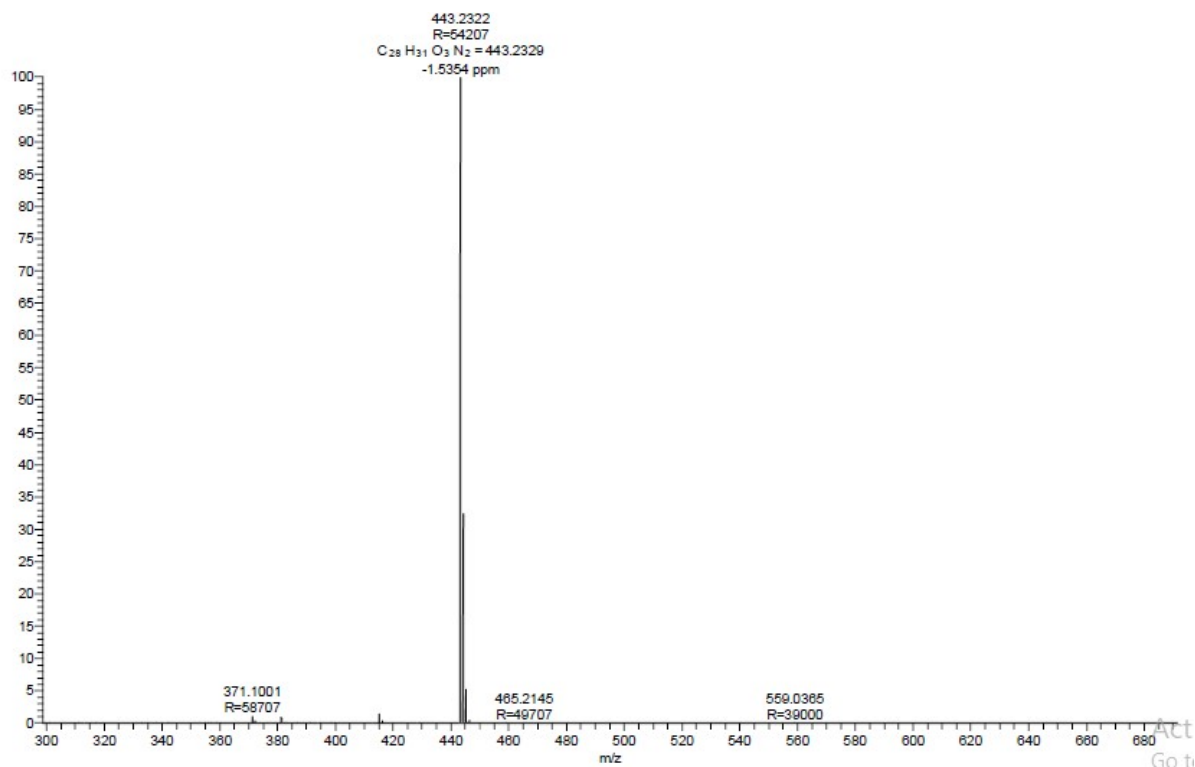


¹³C NMR- of 4,5,6,7-tetrabromo-3',6'-bis(dimethylamino)-3H-spiro[isobenzofuran-1,9'-xanthen]-3-one. (2c)

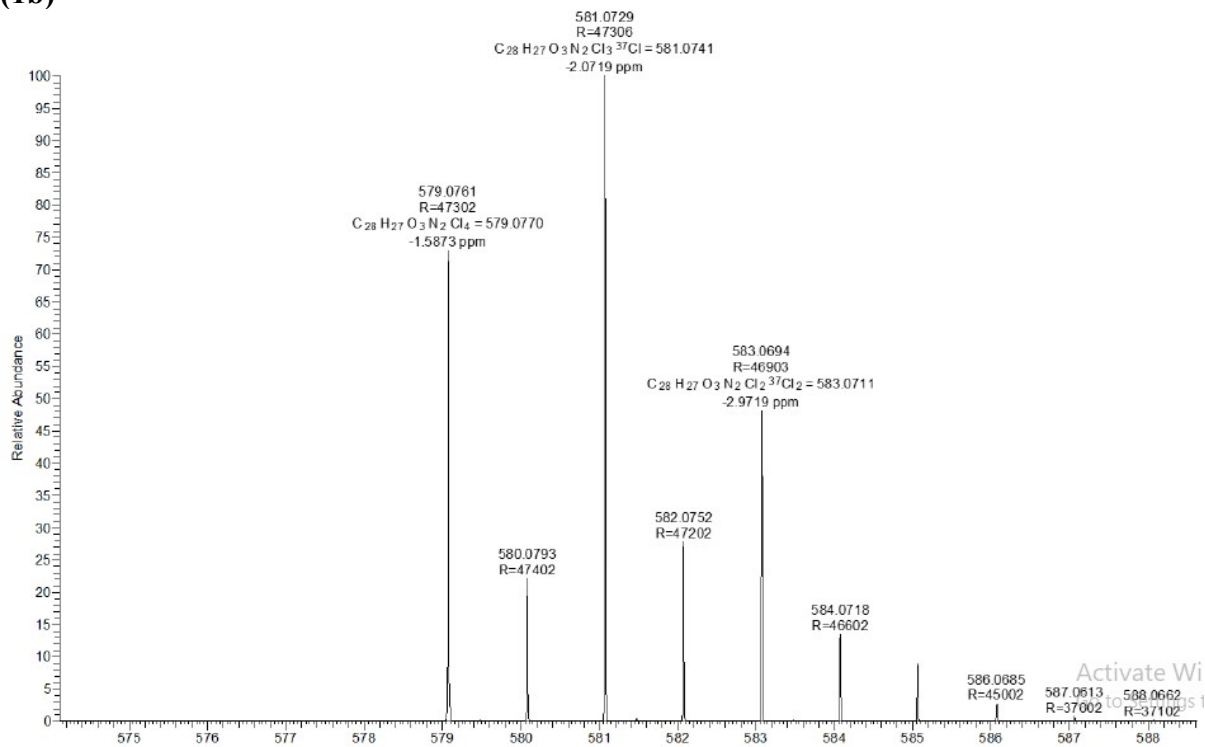


HRMS (High-resolution mass spectrometry) Data

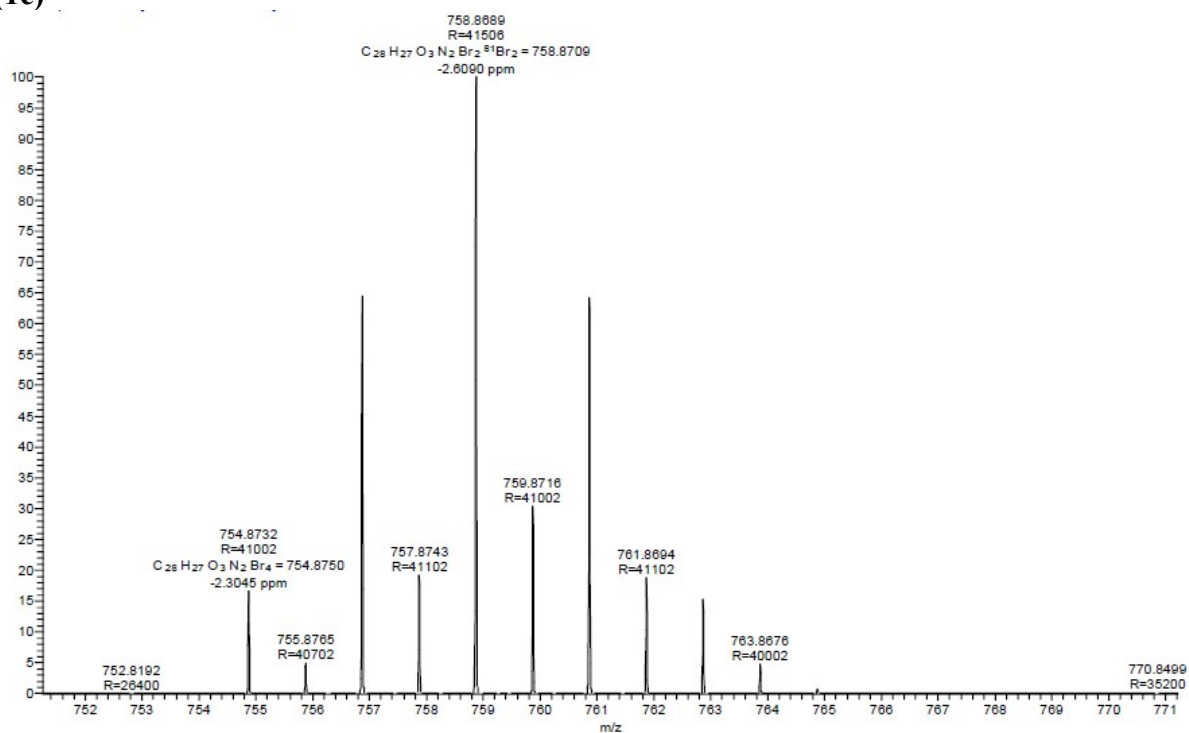
3',6'-bis(diethylamino)-3H-spiro[isobenzofuran-1,9'-xanthen]-3-one. (1a)



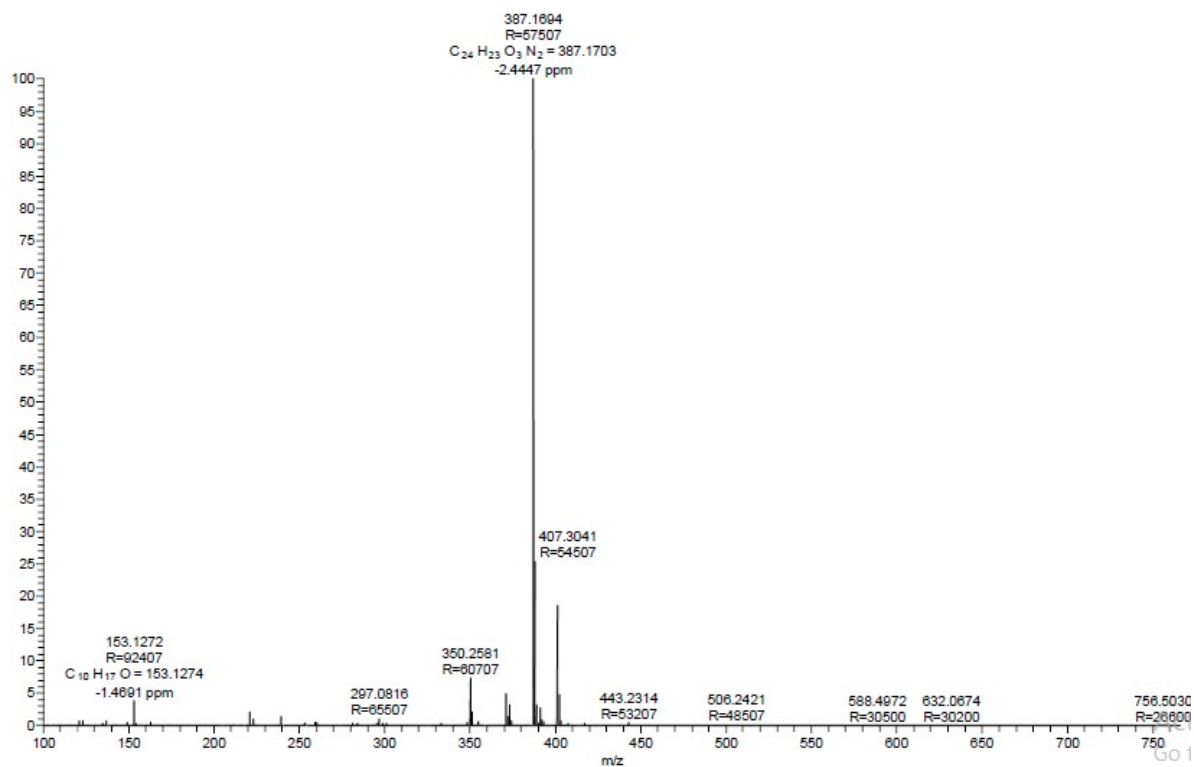
4,5,6,7-tetrachloro-3',6'-bis(diethylamino)-3H-spiro[isobenzofuran-1,9'-xanthen]-3-one. (1b)



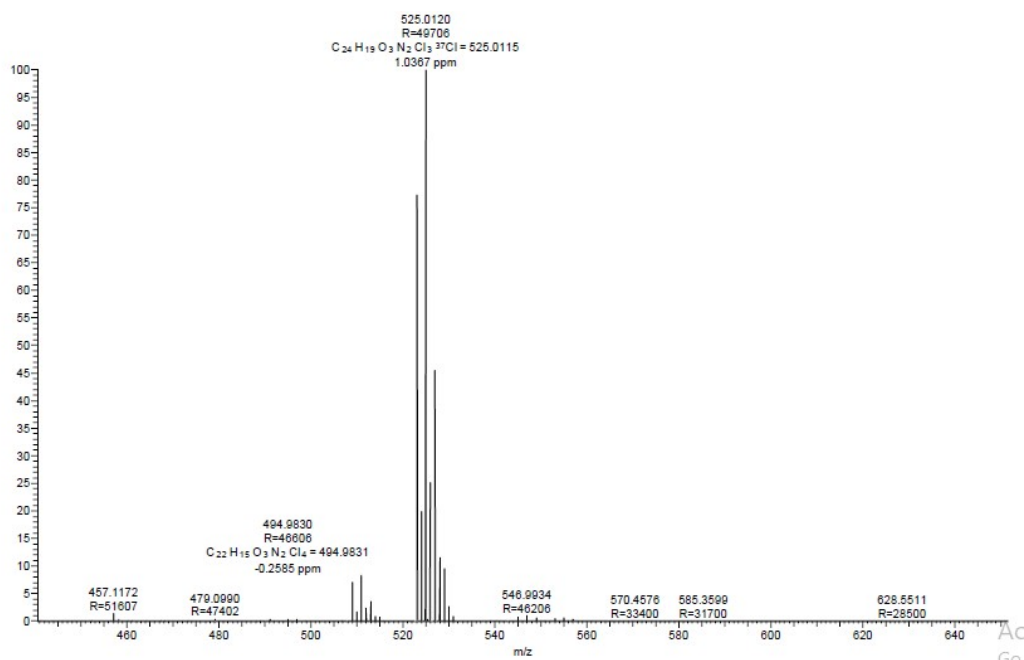
4,5,6,7-tetrabromo-3',6'-bis(diethylamino)-3H-spiro[isobenzofuran-1,9'-xanthen]-3-one. (1c)



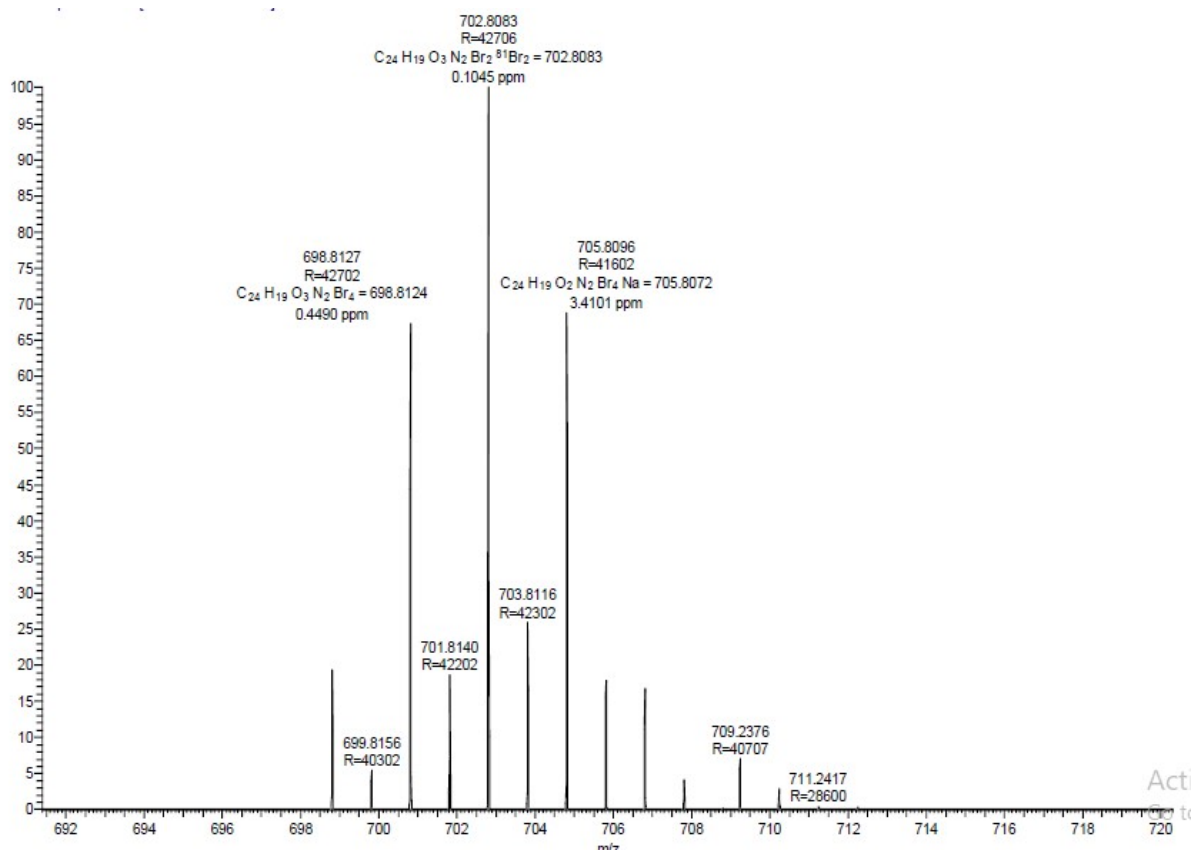
3',6'-bis(dimethylamino)-3H-spiro[isobenzofuran-1,9'-xanthen]-3-one. (2a)



4,5,6,7-tetrachloro-3',6'-bis(dimethylamino)-3H-spiro[isobenzofuran-1,9'-xanthen]-3-one. (2b)



4,5,6,7-tetrabromo-3',6'-bis(dimethylamino)-3H-spiro[isobenzofuran-1,9'-xanthen]-3-one. (2c)



Reference:

- 1 M. Beija, C. A. Afonso and J. M. Martinho, *Chemical Society Reviews*, 2009, **38**, 2410–2433.
- 2 United States, US20050113584A1, 2005.
- 3 K. Kodama, M. Oiwa and T. Saitoh, *Bulletin of the Chemical Society of Japan*, 2021, **94**, 1210–1214.
- 4 G.-S. Jiao, J. C. Castro, L. H. Thoresen and K. Burgess, *Org. Lett.*, 2003, **5**, 3675–3677.
- 5 W. Ming, F. Chen, X. Hu, Z. Zhang, S. Chang, R. Chen, B. Tian and J. Zhang, *Tetrahedron*, 2020, **76**, 131420.
- 6 S. Saha, A. A. Bhosle, A. Chatterjee and M. Banerjee, *J. Org. Chem.*, 2023, **88**, 10002–10013.
- 7 B. H. Sacoman Torquato da Silva, L. Olbera Riehl, G. Carvalho dos Santos, J. Carlos Roldao and L. C. da Silva-Filho, *ChemistrySelect*, 2020, **5**, 1455–1463.
- 8 T. L. Schlick, Z. Ding, E. W. Kovacs and M. B. Francis, *J. Am. Chem. Soc.*, 2005, **127**, 3718–3723.
- 9 D.-Y. Shin, J. Y. Kim and I.-Y. Eom, *Bulletin of the Korean Chemical Society*, 2016, **37**, 2041–2046.
- 10 D. T. Childs, R. A. Hogg, D. G. Revin, I. U. Rehman, J. W. Cockburn and S. J. Matcher, *Applied Spectroscopy Reviews*, 2015, **50**, 822–839.
- 11 O. Aduroja, M. Jani, W. Ghann, S. Ahmed, J. Uddin and F. Abebe, *ACS Omega*, 2022, **7**, 14611–14621.

